Enzymatically-responsive hyaluronan–glucose hydrogel supports MSC survival and preserves paracrine function under glucose deprivation

Gonzalez Fernandez, Paula; Simula, Luca; Jenni, Sébastien; Schvartz, Domitille; Moldovan, Florina; Jordan, Olivier; Allémann, Eric

How to cite

GONZALEZ FERNANDEZ, Paula et al. Enzymatically-responsive hyaluronan–glucose hydrogel supports MSC survival and preserves paracrine function under glucose deprivation. In: International journal of pharmaceutics, 2026, vol. 691, p. 126613. doi: 10.1016/j.ijpharm.2026.126613

This publication URL: https://archive-ouverte.unige.ch/unige:191109
Publication DOI: 10.1016/j.ijpharm.2026.126613

International Journal of Pharmaceutics 691 (2026) 126613

Contents lists available at ScienceDirect

International Journal of Pharmaceutics

journal homepage: www.elsevier.com/locate/ijpharm

Enzymatically-responsive hyaluronan–glucose hydrogel supports MSC survival and preserves paracrine function under glucose deprivation

Paula Gonzalez-Fernandez [a,b], Luca Simula [a,b], Sébastien Jenni [a,b], Domitille Schvartz [c], Florina Moldovan [d], Olivier Jordan [a,b], Eric Allémann [a,b,*]

[a] School of Pharmaceutical Sciences, University of Geneva, Geneva, Switzerland
[b] Institute of Pharmaceutical Sciences of Western Switzerland, University of Geneva, Geneva, Switzerland
[c] Department of Medicine, Faculty of Medicine, University of Geneva, Geneva, Switzerland
[d] Faculty of Pharmacy, Faculty of Dentistry, and CHU Sainte-Justine Research Centre, Université de Montréal, Montréal, QC, Canada

ARTICLE INFO

Keywords:
Starvation
Glucose
Mesenchymal stem cell
Paracrine
Hydrogel
Proteomics

ABSTRACT

Mesenchymal stem cell (MSC) therapy shows potential in regenerative medicine, particularly in treating osteoarthritis (OA). MSCs injected into the joint can secrete growth factors and extracellular matrix molecules, contributing to paracrine communication and cartilage regeneration. However, in the non-vascularized joint environment, MSCs lacking nutrient supply, starve and die too quickly to efficiently deliver enough of these factors. We have recently synthesized a new hydrogel containing hyaluronic acid and glucose (HA-GLC). This hydrogel allows MSCs to survive and proliferate in an environment with otherwise low glucose levels. Furthermore, it releases glucose through enzymatic cleavage by ß-glucosidase, an enzyme which we have shown to be available and active in human bone marrow mesenchymal stem cells (BM-MSCs). In this study, we did incorporate MSCs to this HA-GLC hydrogel. Proteomic analysis of the MSC secretome revealed that glucose deprivation modified the profile of secreted factors, inducing changes in several key pathways, including extracellular matrix production. We then tested the effect of glucose deprivation in MSC secretome on human chondrocyte (hCH) proliferation and IL-6 secretion. Our results showed an increase in hCH proliferation and a significant decrease in IL-6 expression, when cells were exposed to the secretome of MSCs cultured in glucose-provided media rather than glucose-deprived conditions. These findings highlighted the ability of this new technology (HA-GLC hydrogel) to modulate the MSC secretome function, potentially enhancing cartilage regeneration in OA.

1. Introduction

Osteoarthritis (OA) is a chronic progressive joint disease caused by cartilage degeneration and joint inflammation. It leads to pain, swelling, and impaired mobility. OA typically affects knee and hip joints, but it can also impact numerous other joints. Nowadays, treatment modalities focus on pain relief, reducing risk factors, and using walking aids. However, as OA progresses, in some cases arthroplasty may become necessary (Hunter and Bierma-Zeinstra, 2019).

Novel treatments with disease-modifying OA drugs (DMOADs), attempt to slow down or reverse the disease progression. However, no DMOAD is on the market yet (Morici et al., 2024). Stem cell therapy, on the other hand, targets several pathways of cartilage degeneration and has shown promise (Mancuso et al., 2019; Yao et al., 2023). Mesenchymal stem cells (MSCs) secrete beneficial growth factors (such as TGF-ß, FGF-1, BMP-2, MMPs and TIMPs) and induce cartilage regeneration. However, the inflammatory and nutrient-deprived environment makes it hard for the MSCs to survive long enough and exert their therapeutic effect (Giorgino et al., 2023; Gonzalez-Fernandez et al., 2022).

Compared with our previous work describing the synthesis and *in-vitro* validation of HA-GLC as a glucose reservoir, the present study addresses several unanswered and clinically relevant questions (Gonzalez-Fernandez et al., 2024). Here, we investigate if MSC-derived endogenous β-glucosidase can cleave HA-GLC without the need for exogenous enzyme supplementation, thereby mimicking the *in-situ* situation after intra-articular injection. We also investigate how glucose deprivation affects the MSC secretome, which is a crucial mediator of MSC

* Corresponding author at: School of Pharmaceutical Sciences, University of Geneva, Geneva, Switzerland.
E-mail address: eric.allemann@unige.ch (E. Allémann).

https://doi.org/10.1016/j.ijpharm.2026.126613
Received 22 August 2025; Received in revised form 14 January 2026; Accepted 20 January 2026
Available online 23 January 2026

therapeutic effects. It is also investigated if HA-GLC is capable of preserving MSC paracrine activity. This mechanistic and functional characterization was not included in our previous publication and represents the major innovative contribution of the current work.

MSCs need an energy supply. Recently we showed that we were able to efficiently bind glucose covalently to side chains of a hyaluronic acid (HA) polymer backbone. This polymer could then be cleaved by ß-glucosidase to release glucose. Glucose then served as a nutrient for MSCs, as evidenced by the increased viability and proliferation following HA-GLC incubation (Gonzalez-Fernandez et al., 2024). In these experiments, ß-glucosidase was exogenously added to the culture media to ensure cleavage between glucose and the hydrogel.

The rationale for using HA-GLC in osteoarthritis therapy lies in its dual biological role. First, hyaluronic acid acts as a viscoelastic and chondroprotective component of synovial fluid, with well-characterized interactions with MSCs and chondrocytes through the CD44 receptor. Second, the conjugated glucose serves as an enzymatically cleavable nutrient reservoir capable of sustaining MSC metabolic activity when synovial glucose levels are low. By maintaining MSC viability and secretory activity, HA-GLC is expected to enhance the production of anti-inflammatory factors that are essential for cartilage repair, making this technology directly relevant for restoring joint homeostasis in OA.

One of the aims of the present study is to identify endogenous ß-glucosidase in human MSCs. Because glucose uptake is altered in a nutrient-deprived environment (Nuschke et al., 2016), we also wanted to investigate whether the stem cells could benefit from the glucose released by the HA-GLC polymer in a glucose-deprived environment. The ultimate purpose is to characterize and provide a biopolymer that could feed MSCs without requiring a concomitant exogenous enzyme delivery.

In a second part of the present study, we aimed to assess how nutrient deprivation, and particularly the lack of glucose, would influence secretome of MSCs. MSCs therapeutic effects are likely mediated by a paracrine mechanism, due to secretion of exosomes and specific soluble factors such as proteins, lipids, and nucleic acids, the so-called secretome. It has been shown that the secretome can play a key role in intercellular communication, mediating pathological and physiological responses in receiving cells (Zou et al., 2023). We hypothesized that, deprived of nutrients, the MSC secretome would be modified. To address this issue, the secreted proteome of glucose-starved MSCs was analyzed to reveal the potential impact of glucose uptake on the communication between MSCs and neighbouring cells, including chondrocytes.

Indeed, chondrocytes play a crucial role in cartilage synthesis and catabolism. They contribute to the turnover of the extracellular matrix (ECM) in its immediate vicinity (Batushansky et al., 2022; Fujii et al., 2022). In addition, chondrocytes either in direct or indirect contact with MSCs are themselves secreting ECM components such as aggrecan and collagen (Cao et al., 2023; Jiang et al., 2021; Levorson et al., 2014). This led us to investigate how chondrocyte proliferation and IL-6 expression are influenced by MSC secretome under nutrient-deprived conditions compared to a normal nutrient-supplied environment.

In this study, we aimed to characterize the behavior of MSCs in response to a glucose-delivering hyaluronan-based hydrogel (HA-GLC) under nutrient-deprived conditions relevant to the osteoarthritic joint. Specifically, we wanted (i) to confirm whether endogenous β-glucosidase present in MSCs is sufficient to cleave the HA-bound glucose, (ii) to determine whether HA-GLC can sustain MSC glucose uptake and survival in the absence of free glucose, (iii) to evaluate how glucose deprivation alters the MSC secretome and its regenerative and immunomodulatory functions, and (iv) to assess whether HA-GLC can restore these paracrine activities, thereby supporting chondrocyte proliferation and reducing inflammation. Through these objectives, our goal was to establish the therapeutic relevance of HA-GLC as a nutritive, enzyme-responsive hydrogel capable of preserving MSC function in the compromised environment of the OA joint.

2. Materials and methods

2.1. HA-GLC hydrogel synthesis

HA-GLC hydrogel was synthesized as previously described (Gonzalez-Fernandez et al., 2024). Briefly, 4-nitrophenyl-β-D-glucopyranoside was hydrogenated using Pd/C catalyst to obtain 4-aminophenyl-β-D-glucopyranoside. HA was dissolved in distilled water. EDC (5 eq. COO^-), NHS (2 eq. COO^-), and 4-aminophenyl-β-D-glucopyranoside were then added (1 eq. COO^-) and pH was adjusted to 5. After an overnight stirring (12 h) at room temperature (RT), HA-GLC was dialyzed three times against 5 % w/v NaCl (50 kDa MWCO, 4 h, RT) and six times against distilled water (50 kDa, 2 h, RT) before being lyophilized for 72 h at 1.5×10^{-1} mbar and − 80 °C and stored at 4 °C.

2.2. Cells

Bone marrow human Mesenchymal stem cells (hMSC-BM, PromoCell, Germany) were seeded in Mesenchymal stem cell growth medium 2 (PromoCell, Germany) and supplemented with 1 % penicillin–streptomycin (Pen/Strep) until passage 5 (at 37 °C in an atmosphere containing 5 % CO_2). Unless otherwise stated, cells were then treated in a serum-free medium. The different medium conditions for the treatments are listed in the table below (Table 1). Glucose medium (1 g/L), glucose-free medium, glucose-free medium + HA-GLC, glucose-free medium + HA-GLC + ß-glucosidase (20 U/mL), and glucose medium + 10 % FBS. hMSC-BM did not differentiate, CD90, CD73, HLA I, and HLA II markers were tested in the different cell media (Fig. S1). Human chondrocytes (hCH, PromoCell, Germany) were seeded in a chondrocyte growth medium (PromoCell, Germany) and supplemented with 1 % penicillin–streptomycin (Pen/Strep) until passage 5 (at 37 °C in an atmosphere containing 5 % CO2).

2.3. hMSC-BM glucose uptake

hMSC-BM were cultured in a 6 well-plate and the following day, cells were treated in the various medium conditions for 24 h. The cells were washed with phosphate-buffered saline (PBS) and incubated in a glucose-free medium with 37 kBq/mL fluorodeoxyglucose ($[^{18}F]$FDG) (generously provided by the cyclotron, Nuclear medicine department, Geneva University Hospitals) for 60 min at 37 °C, 5 % CO_2. The cells were then washed with PBS and lysed with RIPA cell lysis buffer. FDG uptake was assessed with gamma counter (WIZARD2 2480 Automatic Gamma Counter, Revvity, MA, USA). Results are expressed as counts per minute (cpm) of fluor 18 disintegrations that are linked to glucose. Cell lysate was then quantified by a BCA protein assay kit. Results represent FDG uptake (cpm/µg proteins) relative to the control (DMEM 10 % FBS).

2.4. ß-glucosidase identification

The presence of ß-glucosidase was determined by Western Blot. hMSC-BM cells were cultured on a 6 well-plate and the following day

Table 1
Different media used for cell culture assays on MSCs.

	Medium	Glc (1 g/L)	HA-Glc (20 g/L HA, 1 g/L Glc)	ß-glucosidase (20 U/mL)	FBS (10 %)
A	Glucose	+			
B	Glucose-free				
C	Glucose-free + HA-GLC		+		
D	Glucose-free + HA-GLC + enzyme		+	+	
E	Glucose + FBS	+			+

cells were treated with the same conditions mentioned in Table 1. After 24 h, cells were treated for Western Blot as indicated above, and then incubated overnight at 4 °C with β-glucosidase antibody (B-6) (1:200 in 5 % milk/TBS-T; Santa Cruz Biotechnology, USA). Membranes were washed 3 times for 5 min each with TBS-T, incubated with the goat anti-mouse IgG antibody conjugated to IRDye 800CW (1:10′000 dilution in 5 % milk/TBS-T; LI-COR, USA) for 60 min at RT in the dark, and washed 3 times for 5 min in TBS-T. The membrane was visualized with a 2-channel near-infrared (NIR) fluorescent imager (Odyssey DLx, LI-COR, USA). All membranes were stripped of antibodies and incubated with mouse monoclonal housekeeping antibody vinculin (1:10,000 dilution in blocking solution; Sigma-Aldrich), to normalize the levels of proteins detected. Subsequently a goat anti-mouse IgG antibody conjugated to IRDye 800CW (1:10′000 dilution in 5 % milk/TBS-T; LI-COR, USA) was incubated.

2.5. β-glucosidase activity

The activity of the enzyme was confirmed with the ß-glucosidase activity assay kit (Sigma-Aldrich, USA) according to the supplier's instructions. β-glucosidase activity is assessed by a reaction in which β-glucosidase hydrolyzes p-nitrophenyl-β-D-glucopyranoside leading to the formation of a colored product absorbing at 405 nm, that is proportional to the β-glucosidase activity present in the hMSC-BM lysate. The cell lysate was incubated with the substrate and the initial absorbance was measured. After 20 min, the final absorbance was measured.

2.6. Chondrocytes' proliferation

To determine the effect of hMSC-BM's secretion on hCH proliferation, a WST-1 assay was performed. hCH were plated at an initial 20,000 cells/well density in a 96-well plate and incubated at 37 °C, 5 % CO_2. In parallel, hMSC-BM were seeded at 80 % confluence in a 6 well-plate. The following day, hMSC-BM were treated with the various medium conditions. After 24 h, 50 µL of the hMSC-BM supernatant with the secreted factors was recovered and added to the chondrocytes where the initial medium was replaced with 50 µL of new chondrocytes medium. The chondrocytes were incubated with the hMSC-BM supernatant for 72 h. As controls, we used the chondrocyte's medium and the mesenchymal stem cell medium (without cell secretion). After 72 h the medium was aspirated, and WST-1 reagent (4-[3-(4-iodophenyl)-2-(4-nitrophenyl)–2H-5-tetrazolio]-1,3-benzene disulfonate; Roche, Basel, Switzerland) diluted at a ratio of 1:10 in the medium was added to the cells and incubated 3 h at 37 °C and 5 % CO2. UV absorbance of the samples was measured after 3 h at 450 nm on a plate reader (Biotek, Synergy Mx, Winooski, VT, USA). All measurements were done in triplicate.

2.7. IL-6 expression by hCH

To analyze the effect of hMSC-BM's on hCH under inflammatory condition, the interleukin-6 (IL-6) levels were measured with an enzyme-linked immunosorbent assay (ELISA; Human IL-6 Uncoated ELISA, Thermo Fisher, USA). Chondrocytes were exposed to hMSC-BM supernatant as described in the proliferation assay. The chondrocytes were incubated with the hMSC-BM supernatant and Tumour necrosis factor alpha (TNFα) at 10 ng/mL for 72 h. After the treatment of chondrocytes, culture supernatants were collected, and IL-6 concentration was measured by ELISA according to the supplier's instructions.

2.8. Proteomics analysis

Cells were seeded at 80 % confluence in 9 T75 flasks. The next day, the medium was replaced with 3 different media: glucose-free medium, glucose medium, and HA-GLC in a glucose-free medium. After 24 h the supernatant was recovered and proteins were concentrated with an ultracel 3 kDa regenerated cellulose membrane (15 mL; Sigma-Aldrich, USA). Proteins were then precipitated overnight in trichloroacetic acid (TCA) 100 % at 4 °C. Proteins were centrifuged (20′000 g for 30 min) and washed 3 times with acetone. The supernatant was carefully removed, and the pellet was dried.

Protein extraction and quantification

Cell pellets were resuspended in 50 µL of lysis buffer (0.1 % Rapigest in ammonium bicarbonate 50 mM (BA); Waters, USA). Samples were vortexed 5 min at 95 °C, and sonicated (5 cycles, 70 %, frequency 0.5) with breaks on ice. Afterward, samples were centrifuged (14′000 g for 10 min) and supernatants were recovered after the lysis. BCA assay was used to quantify protein concentrations.

Silver nitrate staining

One µg of proteins were diluted in distilled water up to 6 µL and 4x Laemmli buffer was added to a final volume of 12 µL. Samples were boiled (95 °C) for 5 min and then loaded onto an AccuPAGE™ Tris-Glycine Precast PAGE Gel 4–15 %. Gel electrophoresis was performed at 70 V. To carry out silver nitrate staining, the gel was fixed with a solution of methanol (30 %) and acid acetic (7.5 %) for 1 h. After washing the gel 3 times for 5 min with 10 % ethanol, the gel was incubated for 30 min in a 1 % glutaraldehyde solution. Then, the gel was washed again 5 times and was incubated for 30 min with the silver nitrate solution (0.2 % silver nitrate, 0.28 % Ammoniac (25 %), 0.2 % NaOH 10 N). Once the gel was washed 5 times, it was developed with a citric acid (0.005 %)/ formaldehyde (0.02 %) solution until the reaction was stopped with 1 % acetic acid.

Sample preparation for label-free MS analysis

Samples were heated for 5 min at 95 °C and sonicated (6 x 30 sec.) at 70 % amplitude and 0.5 pulse. Samples were kept 30 sec. on ice between each cycle of sonication then were centrifuged for 10 min. at 14′000 x g. According to the concentration assay, 30 µg (20 µl for samples 7,8,9) of proteins of each sample were digested as follow: sample volume was adjusted to 100 µl with 0.1 % RapiGest in 50 mM AB. Then, 2 µl of Dithioerythritol (DTE) 50 mM were added and reduction was carried out at 37 °C for 1 h. Alkylation was performed by adding 2 µl of iodoacetamide 400 mM during 1 h at room temperature in the dark. Overnight digestion was performed at 37 °C with 6 µL of freshly prepared trypsin (Promega; 0.1 µg/µl in 50 mM AB). To remove RapiGest, samples were acidified with TFA, heated at 37 °C for 45 min. and centrifuged 10 min. at 17′000 x g. Supernatants were then desalted with a C18 microspin column (Harvard Apparatus, Holliston, MA, USA) according to manufacturer's instructions, completely dried under speed-vacuum and stored at −20 °C.

LC-MS/MS

Samples were dissolved 20 µl with loading buffer (5 % CH3CN, 0.1 % FA). Biognosys iRT peptides were added to each sample. 4 µl of peptides were injected on the column. LC-ESI-MS/MS was performed on an Orbitrap Fusion Lumos Tribrid mass spectrometer (Thermo Fisher Scientific) equipped with a Vanquish NEO liquid chromatography system (Thermo Fisher Scientific). Peptides were trapped on a Acclaim pepmap100, C18, 3 µm, 75 µm × 20 mm nano trap-column (Thermo Fisher Scientific) and separated on a 75 µm × 500 mm, C18 ReproSil-Pur (Dr. Maisch GmBH), 1.9 µm, 100 Å, home-made column. The analytical separation was run for 135 min using a gradient of H2O/FA 99.9 %/0.1 % (solvent A) and CH3CN/H2O/FA 80.0 %/19.9 %/0.1 % (solvent B). The gradient was run from 8 % B to 28 % B in 110 min, then to 42 % B in 25 min, then to 95 %B in 5 min with a final stay of 20 min at 95 % B. Flow rate was of 250 nL/min an total run time was of 160 min. Data-Independant Acquisition (DIA) was performed with MS1 full scan at a resolution of 60,000 (FWHM) followed by 30 DIA MS2 scan with sequential fix isolation windows of 28 *m/z* covering a scan range from 400 to 1240 *m/z*. MS1 was performed in the Orbitrap with an AGC target of 1×10^6, a maximum injection time of 50 ms and a scan range from 400 to 1240 *m/z*. DIA MS2 was performed in the Orbitrap using higher-energy collisional dissociation (HCD) at 30 % with an AGC target of 1×10^6 and a maximum injection time of 54 ms.

2.9. Data analysis

Data-Independent Acquisition (DIA) raw files were loaded into Spectronaut v.19 (Biognosys) and analysed by direct DIA using default settings. Briefly, data were searched against homo sapiens reference proteome database (Uniprot, 20′361 entries) combined with an in-house database of common contaminants. Trypsin was selected as the enzyme, with one potential missed cleavage. Variable amino acid modifications were oxidized methionine. Fixed amino acid modification was carbamidomethyl cysteine. Both peptide precursor and protein FDR were controlled at 1 % (Q value < 0.01). Single Hit Proteins were excluded. For quantitation, Protein LFQ method was set to "QUANT 2.0", "only protein group specific" was selected as proteotypicity filter and normalization was performed based on the Local Regression Normalization described by Callister et al. 2006. The quantitative analysis was performed with Spectronaut, proteins were considered to have significantly changed in abundance with an Qvalue ≤ 0.05 and an absolute fold change FC$\geq |2|$ (log2FC $\geq |1|$).

2.10. Statistical and bioinformatic analysis

Data are expressed as mean ± standard deviation (s.d.). The statistical significance of the results was determined using Student's *t*-test (two groups) or one-way analysis of variance (ANOVA, multiple groups) followed by a Tukey test (multiple comparison) in Prism (GraphPad, version 8) with an alpha level of 0.05. P values correspond to *p < 0.05, **p < 0.01, ***p < 0.001, and ****p < 0.0001.

Gene Ontologies term enrichment analysis, as well as associated plots, were performed with ClusterProfiler (G Yu. Thirteen years of clusterProfiler. The Innovation. 2024, 5 (Gonzalez-Fernandez et al., 2022) R package, using the EnrichGO function. Enrichment tests were calculated for GOterms, based on hypergeometric distribution. P-value cutoff was set to 0.05, and Q-value cutoff to 0.01.

3. Results and discussion

To feed MSCs, we synthesized a hyaluronan-based hydrogel, with covalently bound glucose. We have previously shown that the enzymatically triggered biopolymer HA-GLC was able to deliver glucose to MSCs, increasing cell proliferation and survival in starved conditions (Gonzalez-Fernandez et al., 2024). ß-glucosidase catalyzed the hydrolysis of the ß-glycosidic linkage of the ether bond between glucose and HA, leading to glucose release from the HA backbone (Fig. 1). This study demonstrated that if HA-GLC was used at 2 % (w/v), around 1 g/L of glucose was available for the cells. To further explore the potential of this technology, the present study below pursued several goals. First, we aimed to identify endogenous ß-glucosidase in human MSCs and studied their glucose uptake with HA-GLC and in glucose-deprived conditions. Second, we studied how glucose deprivation could influence MSC's secretome and how this secretome could affect neighbouring cells such as chondrocytes. The final goal was to see if the glucose-delivering hydrogel HA-GLC could meet the nutrient needs of MSCs in a glucose-deprived microenvironment such as the joint (Luo et al., 2023).

3.1. ß-glucosidase identification and its activity in MSCs

We have recently shown that the HA-GLC technology could prevent massive stem cell death caused by glucose deprivation (Gonzalez-

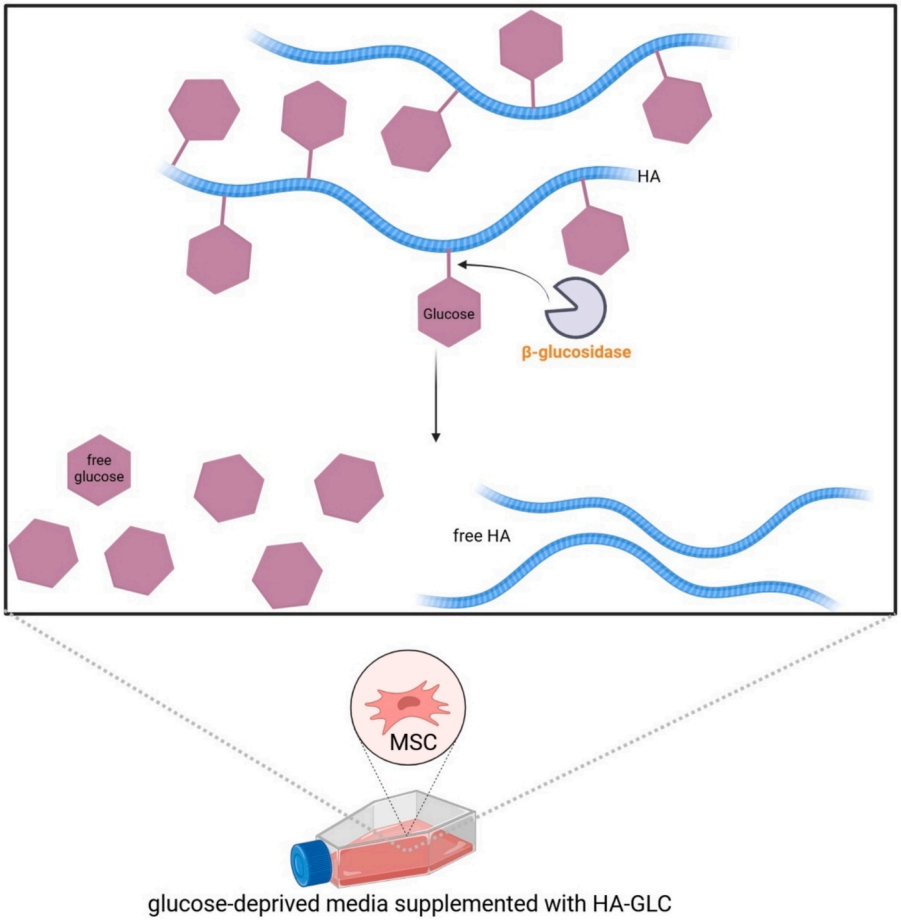

Fig. 1. Schematic representation of HA-GLC hydrogel.

Fernandez et al., 2024). In this previous study, we showed that glucose linked to the hyaluronic acid backbone was indeed released upon exogenous ß-glucosidase addition to the culture, which successfully recognized and cleaved the ether bond between the HA backbone and the side chains bearing glucose molecules (Gonzalez-Fernandez et al., 2024). However, it is crucial for the successful development of the HA-GLC technology to ensure that endogenous enzymes are also capable of cleaving the ß-glycosidic linkage of the ether bond between glucose and HA. To address this, human MSCs were lysed and analyzed to determine whether these cells may be an endogenous source of ß-glucosidase. Actually, the incubation with a ß-glucosidase antibody and western blot analysis established the presence of the endogenous enzyme in MSCs in all conditions, with and without glucose supply, and in the presence of the novel biopolymer HA-GLC (Fig. 2a).

It was already reported that ß-glucosidase was present and even upregulated in inflamed synovial fluid from patients with rheumatoid arthritis (Zhao et al., 2021). Based on this, ß-glucosidase was claimed to be implicated in inflammation by regulating Il-6 production through the p38 signaling (Zhao et al., 2021). In our study, we showed that ß-glucosidase is not only present but also able to recognize and cleave the ether bond between glucose and the backbone of our polymer. This implies that our polymer could sustain for a longer period the viability of injected MSCs by providing a key nutrient, and by using the endogenous ß-glucosidase. It can release glucose *in situ* to feed the cells.

We then characterized ß-glucosidase activity in the presence of HA-GLC. Cell lysates were incubated with a ß-glucosidase substrate (p-nitrophenyl-β-D-glucopyranoside) that can be quantified by a colorimetric assay. Fig. 2b shows that ß-glucosidase activity increased when the cells were incubated together with HA-GLC suggesting that the enzyme was activated when in contact with its substrate (Salgado et al., 2018). The enzyme was identified intracellularly in MSCs, therefore suggesting that glucose was cleaved once HA-GLC was internalized into the cell. The internalization of hyaluronic acid occurs via a well-established CD44 receptor-mediated process and via endocytosis (Knopf-Marques et al., 2016; Kang et al., 2017; Park et al., 2016).

These original data revealed indeed ß-glucosidase presence inside MSCs and its bioactivity when in contact with the added exogenous substrate, HA-GLC polymer. This suggests a potential mechanism for improving MSC proliferation in the presence of glucose supply, or apoptosis in starved conditions, as shown in our previous publication (Gonzalez-Fernandez et al., 2024). To shed light on the process, we therefore characterized the effect of HA-GLC hydrogel in starved conditions on MSCs and the effect of its secretome on inflamed hCH.

To address this point, we investigated: i) glucose uptake in MSCs, ii) the properties of the secretome in starved conditions, and iii) the effect of this secretome on the proliferation and inflammation on hCH, thereby addressing the anti-inflammatory and regenerative properties of MSCs supplemented with HA-GLC in glucose-deprived conditions.

3.2. *MSCs glucose uptake in starved conditions*

To further understand the behaviour of MSCs in the presence or

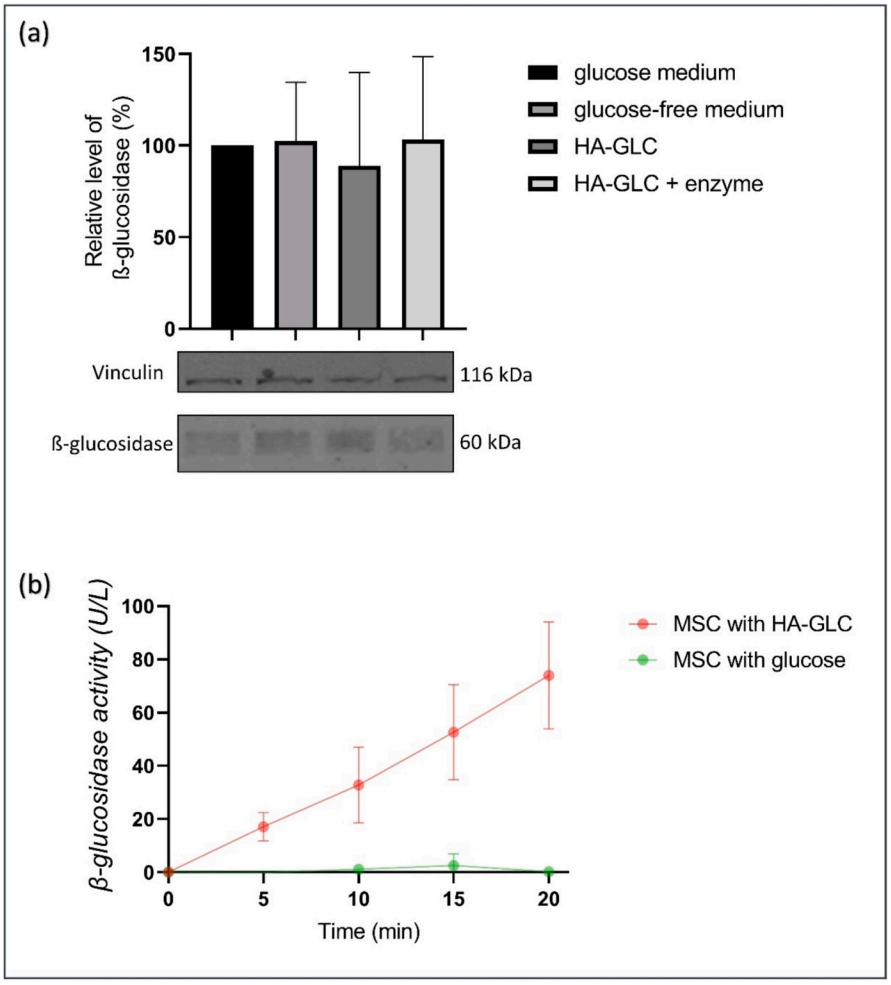

Fig. 2. ß-glucosidase identification and its activity in MSCs. (a) Western blot analysis and quantification of ß-glucosidase protein level. The values were expressed as percentages normalized to the control group (glucose-medium). (b) Enzyme activity was measured by incubating MSC lysate with the enzyme's substrate. The absorbance (405 nm) was measured every 5 min for 20 min (b). Error bars represent the ± standard error of the means of replicates (n = 3).

absence of exogenous glucose, glucose uptake from cells was studied under different conditions. As a control, cells were incubated for 24 h in medium containing FBS (10 %) and 1 g/L of glucose. Results (Fig. 3) were normalized to this control condition, mimicking the best standard environment for healthy cells. When MSCs were starved for 24 h, their glucose uptake was significantly increased (by 4-fold) compared to the control condition where glucose was present in the medium. This indicated also that when cells are deprived of glucose, they take up more glucose to compensate for starvation. This may be due to an overexpression of the GLUT1 receptor preparing the cells to absorb glucose (Nakai et al., 2020; Li et al., 2022). This effect was not observed in the presence of the biopolymer, suggesting that HA-GLC met the glucose needs of MSCs in the absence of glucose in the medium.

It is well known that MSCs injected in an OA joint triggers anti-inflammatory and regenerative pathways through the paracrine mechanism and paracrine intercellular communication (De Bari and Roelofs, 2018). We hypothesized that the composition of secreted factors from MSCs might be affected by starvation conditions. To explore this, the secretome composition was analyzed in starved and non-starved conditions, as well as when the starvation was rescued by the novel biopolymer.

3.3. Proteomic analysis of MSCs secretome

Proteomics analysis of the MSCs secretome was performed by mass spectrometry Data Independent Acquisition (DIA) approach, using protein intensities measured in LC/MS-MS to obtain the resulting relative quantification. MSCs were seeded for 24 h in two different media: a glucose-deprived media and a glucose-provided media. The time point was chosen to guarantee cell survival in the starved cells (Fig. S2). Mass spectrometry analysis allowed quantifying 4207 proteins with at least 2 peptides. The heatmap (Fig. S3) demonstrated a high correlation between the secretome of the same conditions, underlying the homogeneity of replicates preparation. The Venn diagram (Fig. 4a) showed that

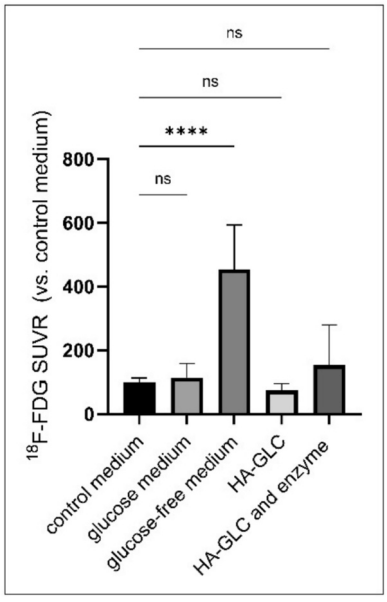

Fig. 3. Average ^{18}F-FDG standardized uptake value ratio (SUVR). Cells were incubated for 24 h, treated with HA-GLC (2 % w/v) and HA-GLC (2 % w/v) with enzymes (ß-glucosidases) in a glucose-free medium. A glucose medium and a glucose-free medium (without FBS) were used as controls. The control medium is provided with FBS 10 %. Values represent intracellular activity (^{18}F-FDG uptake/µg protein relative to a control medium with 10 % FBS. Experiments were performed as independent triplicates. Error bars represent the ± standard error of the means of replicates. * $p < 0.05$, ** $p < 0.01$, *** $p < 0.001$, **** = $p < 0.0001$.

3357 proteins were commonly identified into the 2 conditions, with 818 proteins being exclusive to glucose neg (glucose-deprived media) and 32 to glucose pos (glucose-provided media). Differentially expressed proteins (fold-change $> \pm 2$, q-value $\leq 0{,}05$) were displayed in blue in a volcano plot (Fig. 4b). The volcano plot gave a global visualization of the quantitative changes in the secreted proteins when MSCs are deprived of glucose. Proteins that were quantified in at least two samples of each condition were considered for GO analysis (1147 proteins). The GO analysis grouped the results as per biological process and cellular component. The most significantly enriched terms are represented in Fig. 5.

The Top 15 enriched cellular components (p-value $<$ 2E-13) were illustrated in a cnet plot (Fig. 5a). Each dot represented a protein, and the colour indicated the fold-change. Green dots are down-regulated proteins from glucose-deprived media and red dots are up-regulated proteins in glucose-deprived media. The Cellular Component enrichment pointed out that the most enriched terms are associated with collagen-containing extracellular matrix, endoplasmic reticulum lumen, basement membrane, vacuolar lumen, lysosomal lumen and platelet alpha granule lumen. The secreted proteins associated with these terms were mainly down-regulated in the starved condition. However, proteins associated with the enriched terms “cytosolic ribosome” and “focal adhesion” were found significantly up-regulated (red dots). These proteins being mostly intracellular, their presence in the medium implies a leakage from the cell’s cytosol and may indicate cell death.

Similar results were observed when matching the proteins to GO of Biological processes. The Top 15 enriched biological processes (p-value $<$ 3.2E−13) were illustrated in a cnet plot (Fig. 5b). Representative proteins of various biological processes, such as aminoglycan metabolic process, glycosaminoglycan metabolic process, connective tissue development, glycoprotein metabolic process, proteoglycan metabolic process, collagen metabolic process, extracellular structure organization, and wound healing were found down-regulated in the glucose-deprived condition. Basically, the proteins involved in the processes from regeneration and extracellular matrix construction are down-regulated when MSCs are starved. The enrichment of intracellular processes were also highlighted with these results, as “cytoplasmic translation” and “ribonucleoprotein complex biogenesis”. The associated proteins were significantly up-regulated, suggesting that cell death happened.

During starvation, MSCs are in stressed conditions and the whole secretome seemed to be affected, secreting significantly less factors involved in regeneration and ECM processes. Cell death during starvation was also observed. It has already been reported that in mammalian cells, stress conditions lead to a complex reprogramming of cellular processes, generally resulting in a suppression of secretion pathways to conserve resources and maintain cellular homeostasis (van Leeuwen et al., 2018; Nüchel et al., 2021; Bhowmick et al., 2024). In the context of OA, MSC therapy is of interest because of the different therapeutic factors they secrete in an injured site (Gonzalez-Fernandez et al., 2022; Han et al., 2022; Xiang et al., 2022). We therefore selected a few of these proteins (Table 2) and had a closer look to how starvation influenced their secretion.

Proteins that are key players in the therapeutic effect of MSCs and found down-regulated or absent in the secretome of glucose-deprived media are listed in Table 2. An important axis of MSC’s therapeutic effect is the ECM remodelling and the increase of chondrocyte proliferation during OA (De Bari and Roelofs, 2018). Several secreted factors involved in these pathways were found significantly down-regulated in the secretome of MSCs exposed to glucose-deprived media such as: MMP-1, MMP-2, TIMP-1, TIMP-2, COL2A1, HGF and FGF-1. Metalloproteinases (MMP) and tissue-inhibitors-of-matrix-metalloproteinases (TIMP) are both secreted by MSCs in a controlled manner. There are different MMPs in OA, but MMP-1 is responsible of degrading fibrotic collagen (collagen I and III) and MMP-2 targeting type IV collagen. TIMPs regulate the activity of MMPs and there is a precise balance of

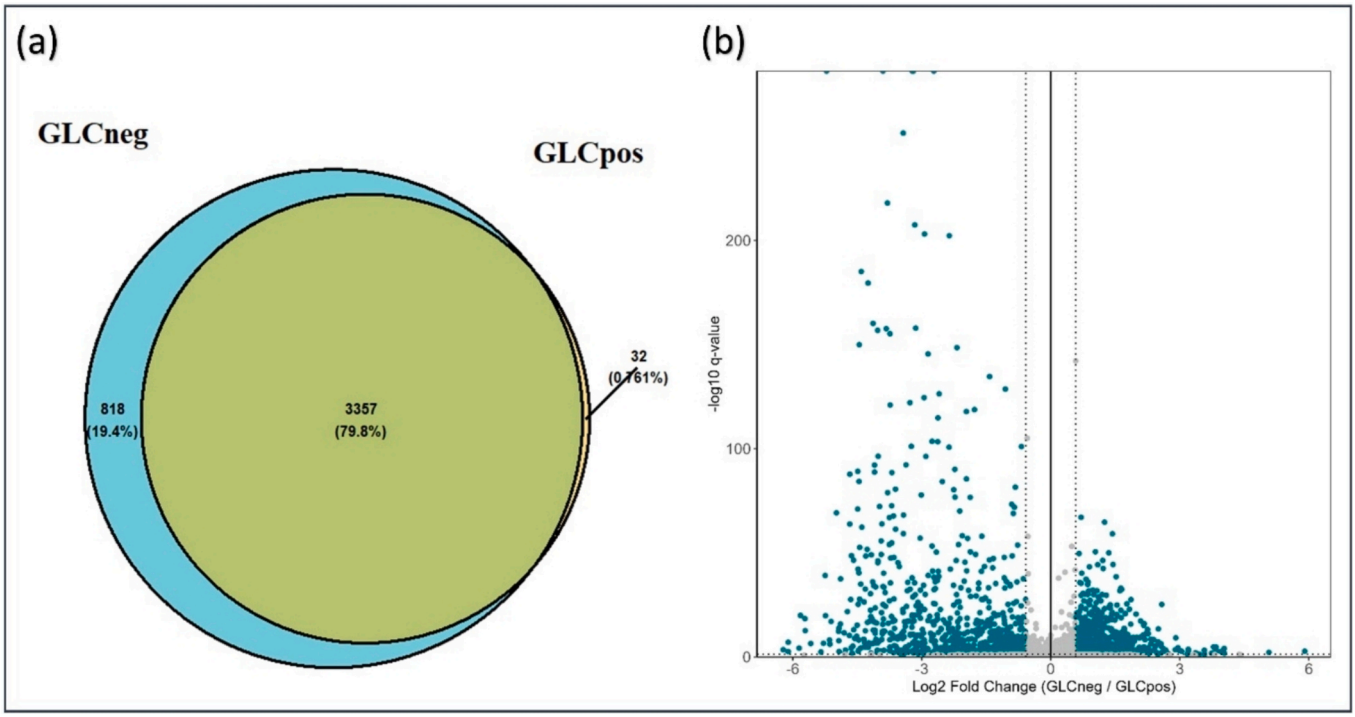

Fig. 4. Venn diagram and volcano plot of protein expression of MSCs secretome in glucose-deprived (GLCneg) versus glucose-provided conditions (GLCpos). The Venn diagram of proteins quantified with at least 2 peptides (a). Volcano plot was constructed using $\log_2$ fold change and $-\log_{10}$ q-value. The blue dots represent the differentially expressed proteins (fold-change $> \pm$ 2, q-value $\leq$ 0.05) between glucose-provided and glucose-deprived cells (b).

secretion between these enzymes ensuring ECM modelling by MSCs (Rose and Kooyman, 2016; Almalki and Agrawal, 2016; Burk et al., 2022). In our study, TIMP-1, TIMP-2, MMP-1, and MMP-2 were found significantly down-regulated in MSC's secretome obtained with glucose-deprived media. Collagen type II (COL2A1) was also found down-regulated by 10-fold compared to the glucose-provided media secretome. Collagen type II is one of the key components of the ECM of cartilage. These findings suggested that starvation in MSCs may impair the balance between these collagen-degrading enzymes.

Transforming growth factor ß 1 (TGFß-1) contributes to cartilage homeostasis and repair but also to disease progression during OA when dysregulated. TGFß-1 regulates chondrocytes proliferation and ECM anabolism in stem cells (Ying et al., 2018; Xu et al., 2018). The secretion of this cytokine is therefore crucial for keeping the microenvironment of the joint healthy. In glucose-deprived conditions, TGFß-1 was found significantly down-regulated by 13.7-fold.

Another key therapeutic effect of MSCs is their anti-inflammatory and immunomodulatory effect in OA. Cytokines such as HGF, PGE-2 and IL-6 are released by MSCs to reduce and regulate inflammation (Bouffi et al., 2010; Tonomura et al., 2020). We found here that the secretion of these cytokines is significantly reduced when MSCs are glucose-deprived. These results suggested that the anti-inflammatory therapeutic effect of MSCs is impaired during starvation.

It is of interest to note that two very interesting proteins were absent in the secretome of the glucose-deprived condition: i) Bone morphogenetic protein 2 (BMP-2) and ii) Protein APCDD1-like. BMP-2 plays a crucial role in cartilage homeostasis and repair and has been widely studied as a potential disease-modifying osteoarthritis drug (DMOAD) candidate (Deng et al., 2018). It has already been tested in various osteoarthritic animal models to study their effect on cartilage regeneration (Blaney Davidson et al., 2007; Glansbeek et al., 1997). Interestingly, BMP-2 was not detected in the glucose-deprived secretome, suggesting that glucose availability may be essential for BMP-2 secretion and potential cartilage-repairing functions.

In contrast to the BMP-2, little is known about the role of APCDD1 in OA. This extracellular glycoprotein is a therapeutic target in vascular disease, cardiac diseases, the nervous system and the skin (Vonica et al., 2020; Foulquier et al., 2018). The protein's biological potential is due to its ability to inhibit the WNT signalling pathway, particularly the WNT/ß-catenin signalling pathway, where WNT binds to transmembrane receptors (Frizzled/LRP5) which activate ß-catenin that enters the nucleus and promotes cell growth, differentiation, and proliferation (Clevers, 2006). However, in OA, excessive activation of the WNT/ß-catenin contributes to the development of OA-like phenotype chondrocytes and promotes inflammation (Zhu et al., 2009). Given its role in OA disease, this pathway is a promising therapeutic target with pharmacological inhibitors, such as Lorecevivint, currently being investigated (Cheng et al., 2022). Since ACDD1 inhibits WNT/ß-catenin signalling pathway, it could represent a new therapeutic target in OA. However, the absence of this protein in the glucose-deprived secretome suggested that glucose may be necessary for its secretion and potential WNT pathway inhibition.

A qualitative proteomic analysis of the MSCs secretome treated with HA-GLC hydrogel was performed. When comparing the proteins specific of the glucose-deprived condition (not identified into the glucose-provided condition) with those of the HA-GLC condition, only 10 out of 818 proteins (1,2 %) were commonly identified between both conditions (Fig. 6a). However, when comparing the proteins specific of the glucose-provided condition with those in the HA-GLC condition, 12 out of 32 proteins (37 %) were found in both samples (Fig. 6b). These findings suggested that the proteomic profile of HA-GLC-treated MSCs is closer to the glucose-provided condition. Since MSCs were incubated in a glucose-deprived medium supplemented with HA-GLC, these results indicated that the hydrogel provided the glucose needs, preventing alterations in secretome composition. Furthermore, when ranking the 15 most abundant proteins in the secretome of the HA-GLC conditions, almost only extracellular proteins were found, such as, TIMP-1, MMP-2 and Collagen type I, suggesting minimal or no cell death in this condition (Fig. S4).

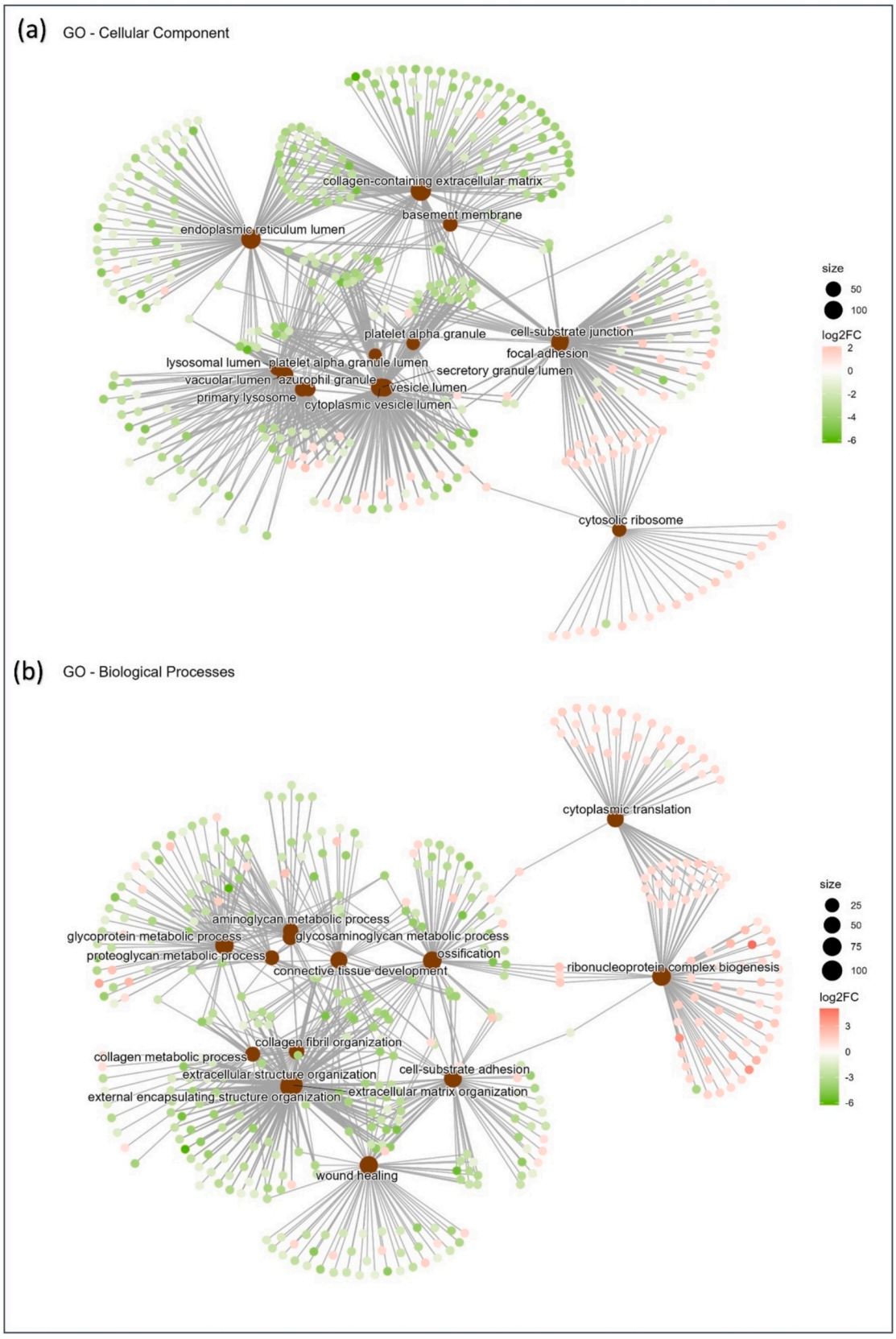

Fig. 5. Representation of the top 15 GO terms enriched (biological processes and cellular component) in MSC secretome. LC/MS-MS data were analyzed and differentially expressed proteins were matched to GO databases. Protein fold-change are represented as follows: The red dots are up-regulated proteins in the glucose-deprived media, and the green dots are down-regulated proteins in the glucose-deprived media.

Table 2
Key secreted proteins from MSCs during OA found down-regulated in glucose-deprived media. (* proteins identified only in 1 out of 3 replicates of glucose neg).

ProteinGroups	Protein descriptions	Genes	AVG Log2RatioNeg/Pos	Qvalue Neg/Pos
P08253	72 kDa type IV collagenase	MMP2	−4,45	1,23E-150
P03956	Interstitial collagenase	MMP1	−4,02	5,11E-46
P01137	Transforming growth factor beta-1 proprotein	TGFB1	−3,78	6,42E-17
P01033	Metalloproteinase inhibitor 1	TIMP1	−3,75	1,05E-27
P11362	Fibroblast growth factor receptor 1	FGFR1	−3,74	1,22E-3
P16035	Metalloproteinase inhibitor 2	TIMP2	−3,72	3,23E-48
P14210	Hepatocyte growth factor	HGF	−3,63	2,9E-18
P02458	Collagen alpha-1(II) chain	COL2A1	−3,33	8,53E-6
P40189	Interleukin-6 receptor subunit beta	IL6ST	−3	9,23E-6
P12643	Bone morphogenetic protein 2	BMP2	−1,63*	1,51E-2
Q8NCL9	Protein APCDD1-like	APCDD1L	−1,6*	2,5E-2
Q9H7Z7	Prostaglandin E synthase 2	PTGES2	−1,24	2,24E-2

3.4. MSCS secretome effect on chondrocyte proliferation and IL-6 expression

We finally looked at the anti-inflammatory and regenerative potential of MSCs in the glucose-deprived environment in presence of the polymer HA-GLC. The MSC medium is serum-free to deprive the cells of nutritional support (Nuschke et al., 2016; Ferro et al., 2019). MSC's supernatant (cell secretome) was added to the chondrocytes and its impact on proliferation and inflammation was analyzed. For the assessment of chondrocyte proliferation, we measured mitochondrial dehydrogenase activity. Chondrocytes were exposed to the different MSC's secretome for 72 h. MSC medium (with serum and glucose) is used as a control on chondrocytes.

The results in Fig. 7a showed that the proliferation of hCH exposed to MSCs secretome and HA-GLC was not only restored, but even higher compared to the chondrocyte medium ($p = 0.0026$). The control in standard MSC medium decreased proliferation by about 20 % compared to the control with a standard chondrocyte medium. Furthermore, the secretome of MSCs that were fed with glucose released by HA-GLC, was as performant as the glucose medium condition. A less important proliferation increase of hCH was observed in a glucose *vs* glucose-free condition (111 % *vs* 79 %, $p = 0.0076$) highlighting the importance of a nutrient-supplied environment for cell interaction (Denoeud et al., 2023; Moya et al., 2018). These findings are essential as there is a low glucose amount available in synovial fluids. hCH proliferation was significantly restored in all conditions. Proliferation was more than 100 % for all conditions except for the secretome treated in a glucose-free medium. These results outline an important therapeutic potential of MSCs used for cell therapy: the paracrine communication. MSCs secrete factors to interact with other cells, such as chondrocytes and inflammatory cells (Mancuso et al., 2019). Other studies also show an increase in proliferation when chondrocytes are in contact either directly with MSCs or its secretome (Yang et al., 2024; Jammes et al., 2023). In this study, we added the factors to assess how the secretome of glucose-deprived MSCs is affecting hCH. The HA-GLC technology could therefore restore a nutrient-deprived environment by releasing glucose from the hydrogel. The proliferation rate of hCH exposed to HA-GLC was comparable to that of cells cultured in a glucose-supplemented medium, suggesting that HA-GLC hydrogel supports cell growth under glucose-deprived conditions.

Beyond cell proliferation, we also studied the effect on hCH inflammation. To address this, we measured the IL-6 expression by ELISA (Fig. 7b). Chondrocytes were pre-treated with TNFα (10 ng/mL) and then incubated with the media containing the MSC's secretome. The results in Fig. 3b showed that IL-6 levels doubled after TNFα treatment. After adding the MSC's secretome, a decrease was observed in all conditions except for the secretome treated in a glucose-free medium. Our results showed the importance of glucose to stimulate the secretion of the anti-inflammatory factors of the MSC secretome. Specifically, the HA-GLC demonstrated a 2-fold decrease of chondrocytes' IL-6 production ($p = 0.0058$). Recently, similar results were reported for the effect of human umbilical cord derived MSCs on synovial fluid, chondrocytes, and in a rat OA model (Yang et al., 2024). A decrease of inflammatory factors, such as IL-6 was also observed, thus indicating the importance of MSC-secretome that offer a promising option for OA therapy.

Taken together, these findings emphasize that the availability of glucose is a crucial determinant of MSC therapeutic performance. Starvation profoundly altered the MSC secretome, suppressing ECM-related proteins, growth factors and anti-inflammatory mediators. HA-GLC effectively prevented this collapse by sustaining glucose metabolism, thereby preserving MSC paracrine signaling. This is particularly relevant in the osteoarthritic joint, where synovial glucose is significantly lower than in blood. By acting both as a viscoelastic HA carrier and as an endogenous enzyme-responsive glucose reservoir, HA-GLC addresses a key limitation of MSC therapy and may significantly improve its clinical efficacy.

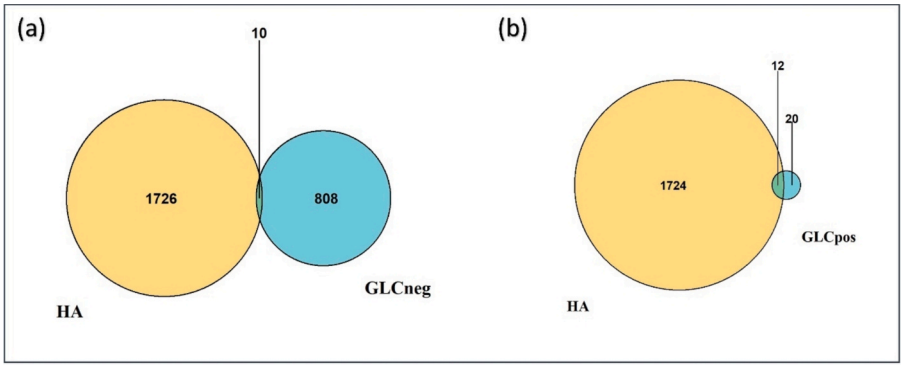

Fig. 6. Venn diagram illustrating (a) proteins specific to the glucose-deprived condition (GLCneg) and the HA-GLC condition, and (b) proteins exclusive to the glucose-provided condition (GLCpos) and the HA-GLC condition.

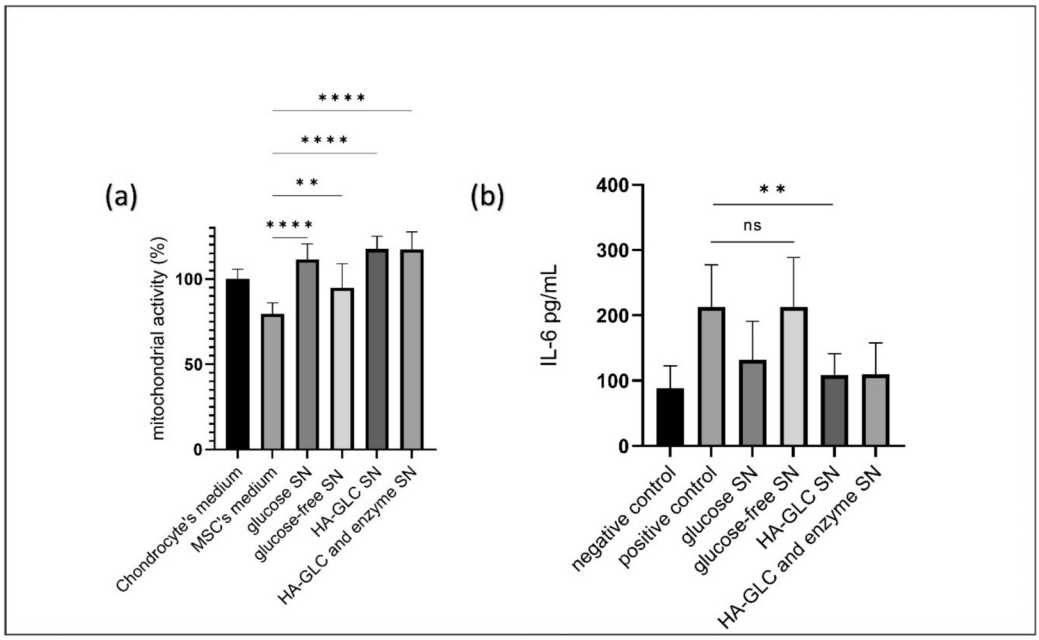

Fig. 7. Effect of MSC' supernatant secretome on chondrocyte (a) proliferation by WST-1 assay and (b) inflammation by IL-6 ELISA analysis. MSCs were incubated in different media: a glucose medium, a glucose-free medium, a glucose-free medium with HA-GLC hydrogel, a glucose-free medium with HA-GLC hydrogel, and a glucose-free medium with HA-GLC hydrogel and enzymes. After 24 h, the supernatant (SN) of each condition was recovered and added to the previously seeded chondrocytes for 72 h. WST-1 reagent was added for cell proliferation and mitochondrial activity was measured (a). For the Il-6 analysis, chondrocytes were treated with TNFα 10 ng/ml and the MSC supernatant and inflammation was measured by ELISA (b). Experiments were performed as independent triplicates. Error bars represent the ±standard error of the means of replicates. * $p < 0.05$, ** $p < 0.01$, *** $p < 0.001$, **** = $p < 0.0001$.

4. Conclusions

We first demonstrated here the presence of the enzyme ß-glucosidase in MSCs, which would allow glucose delivery without the need for adding exogenous enzymes to the injected MSCs and polymer. The glucose moiety was successfully cleaved from the HA backbone, and the glucose uptake profile of MSCs was similar under conditions with glucose or with the hydrogel deprived of glucose. Therefore, the glucose cleaved from the polymer was sufficient to meet the MSCs' glucose needs.

This study identified the secreted proteins from MSCs incubated with and without glucose. Significant differences were observed in the enriched biological processes and cellular components between the two conditions. Without glucose, the profile of secreted proteins was highly altered into pathways such as GAG, collagen and proteoglycan production. The proteins belonging to these specific pathways were found down-regulated when cells were starved. In contrast, proteins associated to ribosomes were significantly up-regulated in glucose-starved MSCs, suggesting an early stage of cell apoptosis.

Additionally, MSCs communication with neighbouring hCH was assessed by evaluating their proliferation and inflammation response following exposure to the MSC secretome. Chondrocyte proliferation increased significantly, and the IL-6 expression decreased.

Overall, these findings highlighted that the polymer's glucose was sufficient to sustain MSCs without the need for exogenous enzymes. The proteomic analysis further illustrated glucose's role in ECM production. Our hydrogel HA-GLC appears to meet the nutrient needs of MSCs, enabling continued paracrine signaling, and promoting biological factors necessary for cartilage anabolism and regeneration.

CRediT authorship contribution statement

Paula Gonzalez-Fernandez: Writing – original draft, Visualization, Validation, Methodology, Investigation, Formal analysis, Data curation, Conceptualization. **Luca Simula:** Methodology, Investigation, Conceptualization. **Sébastien Jenni:** Investigation. **Domitille Schvartz:** Methodology, Formal analysis, Data curation. **Florina Moldovan:** Writing – review & editing. **Olivier Jordan:** Writing – review & editing, Validation, Supervision, Methodology, Formal analysis, Conceptualization. **Eric Allémann:** Writing – review & editing, Validation, Resources, Project administration, Methodology, Formal analysis, Conceptualization.

Declaration of competing interest

The authors declare that they have no known competing financial interests or personal relationships that could have appeared to influence the work reported in this paper.

Acknowledgements

We thank the financial support provided by the Swiss National Science Foundation (SNSF) project 205321_184936.

Appendix A. Supplementary material

Supplementary data to this article can be found online at https://doi.org/10.1016/j.ijpharm.2026.126613.

Data availability

We have shared a DOI link to our data repository

References

Almalki, S.G., Agrawal, D.K., 2016. Effects of matrix metalloproteinases on the fate of mesenchymal stem cells. Stem Cell Res Ther 7 (1), 129.

Batushansky, A., Zhu, S., Komaravolu, R.K., South, S., Mehta-D'souza, P., Griffin, T.M., 2022. Fundamentals of OA. An initiative of osteoarthritis and cartilage. obesity and metabolic factors in OA. Osteoarthritis Cartilage 30 (4), 501–515.

Bhowmick, T., Biswas, S., Mukherjee, A., 2024. Cellular response during cellular starvation: a battle for cellular survivability. Cell Biochem. Funct. 42 (5), e4101.

Blaney Davidson, E.N., Vitters, E.L., van Lent, P.L., van de Loo, F.A., van den Berg, W.B., van der Kraan, P.M., 2007. Elevated extracellular matrix production and degradation upon bone morphogenetic protein-2 (BMP-2) stimulation point toward a role for BMP-2 in cartilage repair and remodeling. Arthritis Res. Ther. 9 (5), R102.
Bouffi, C., Bony, C., Courties, G., Jorgensen, C., Noël, D., 2010. IL-6-dependent PGE2 secretion by mesenchymal stem cells inhibits local inflammation in experimental arthritis. PLoS One 5 (12), e14247.
Burk, J., Sassmann, A., Kasper, C., Nimptsch, A., Schubert, S., 2022. Extracellular matrix synthesis and remodeling by mesenchymal stromal cells is context-sensitive. Int. J. Mol. Sci. 23 (3).
Cao, H., Chen, M., Cui, X., Liu, Y., Liu, Y., Deng, S., et al., 2023. Cell-free osteoarthritis treatment with sustained-release of chondrocyte-targeting exosomes from umbilical cord-derived mesenchymal stem cells to rejuvenate aging chondrocytes. ACS Nano 17 (14), 13358–13376.
Cheng, J., Li, M., Bai, R., 2022. The Wnt signaling cascade in the pathogenesis of osteoarthritis and related promising treatment strategies. Front. Physiol. 13, 954454.
Clevers, H., 2006. Wnt/beta-catenin signaling in development and disease. Cell 127 (3), 469–480.
De Bari, C., Roelofs, A.J., 2018. Stem cell-based therapeutic strategies for cartilage defects and osteoarthritis. Curr. Opin. Pharmacol. 40, 74–80.
Deng, Z.H., Li, Y.S., Gao, X., Lei, G.H., Huard, J., 2018. Bone morphogenetic proteins for articular cartilage regeneration. Osteoarthritis Cartilage 26 (9), 1153–1161.
Denoeud, C., Luo, G., Paquet, J., Boisselier, J., Wosinski, P., Moya, A., et al., 2023. Enzyme-controlled, nutritive hydrogel for mesenchymal stromal cell survival and paracrine functions. Commun. Biol. 6 (1), 1266.
Ferro, F., Spelat, R., Shaw, G., Duffy, N., Islam, M.N., O'Shea, P.M., et al., 2019. Survival/adaptation of bone marrow-derived mesenchymal stem cells after long-term starvation through selective processes. Stem Cells 37 (6), 813–827.
Foulquier, S., Daskalopoulos, E.P., Lluri, G., Hermans, K.C.M., Deb, A., Blankesteijn, W. M., 2018. WNT signaling in cardiac and vascular disease. Pharmacol. Rev. 70 (1), 68–141.
Fujii, Y., Liu, L., Yagasaki, L., Inotsume, M., Chiba, T., Asahara, H., 2022. Cartilage homeostasis and osteoarthritis. Int. J. Mol. Sci. 23 (11).
Giorgino, R., Albano, D., Fusco, S., Peretti, G.M., Mangiavini, L., Messina, C., 2023. Knee osteoarthritis: epidemiology, pathogenesis, and mesenchymal stem cells: what else is new? An update. Int. J. Mol. Sci. 24 (7).
Glansbeek, H.L., van Beuningen, H.M., Vitters, E.L., Morris, E.A., van der Kraan, P.M., van den Berg, W.B., 1997. Bone morphogenetic protein 2 stimulates articular cartilage proteoglycan synthesis in vivo but does not counteract interleukin-1alpha effects on proteoglycan synthesis and content. Arthritis Rheum. 40 (6), 1020–1028.
Gonzalez-Fernandez, P., Rodríguez-Nogales, C., Jordan, O., Allémann, E., 2022. Combination of mesenchymal stem cells and bioactive molecules in hydrogels for osteoarthritis treatment. Eur. J. Pharm. Biopharm. 172, 41–52.
Gonzalez-Fernandez, P., Simula, L., Jenni, S., Jordan, O., Allémann, E., 2024. Hyaluronan-based hydrogel delivering glucose to mesenchymal stem cells intended to treat osteoarthritis. Int. J. Pharm. 657, 124139.
Han, Y., Yang, J., Fang, J., Zhou, Y., Candi, E., Wang, J., et al., 2022. The secretion profile of mesenchymal stem cells and potential applications in treating human diseases. Signal Transduct. Target. Ther. 7 (1), 92.
Hunter, D.J., Bierma-Zeinstra, S., 2019. Osteoarthritis. Lancet 393 (10182), 1745–1759.
Jammes, M., Contentin, R., Audigié, F., Cassé, F., Galéra, P., 2023. Effect of pro-inflammatory cytokine priming and storage temperature of the mesenchymal stromal cell (MSC) secretome on equine articular chondrocytes. Front. Bioeng. Biotechnol. 11, 1204737.
Jiang, S., Tian, G., Yang, Z., Gao, X., Wang, F., Li, J., et al., 2021. Enhancement of acellular cartilage matrix scaffold by Wharton's jelly mesenchymal stem cell-derived exosomes to promote osteochondral regeneration. Bioact. Mater. 6 (9), 2711–2728.
Kang, M.L., Jeong, S.Y., Im, G.I., 2017. Hyaluronic acid hydrogel functionalized with self-assembled micelles of amphiphilic PEGylated kartogenin for the treatment of osteoarthritis. Tissue Eng. A 23 (13–14), 630–639.
Knopf-Marques, H., Pravda, M., Wolfova, L., Velebny, V., Schaaf, P., Vrana, N.E., et al., 2016. Hyaluronic acid and its derivatives in coating and delivery systems: applications in tissue engineering, regenerative medicine and immunomodulation. Adv. Healthc. Mater. 5 (22), 2841–2855.
Levorson, E.J., Santoro, M., Kasper, F.K., Mikos, A.G., 2014. Direct and indirect co-culture of chondrocytes and mesenchymal stem cells for the generation of polymer/extracellular matrix hybrid constructs. Acta Biomater. 10 (5), 1824–1835.
Li, R., Kato, H., Taguchi, Y., Umeda, M., 2022. Intracellular glucose starvation affects gingival homeostasis and autophagy. Sci. Rep. 12 (1), 1230.
Luo, G., Wosinski, P., Salazar-Noratto, G.E., Bensidhoum, M., Bizios, R., Marashi, S.A., et al., 2023. Glucose metabolism: optimizing regenerative functionalities of mesenchymal stromal cells postimplantation. Tissue Eng. B Rev. 29 (1), 47–61.
Mancuso, P., Raman, S., Glynn, A., Barry, F., Murphy, J.M., 2019. Mesenchymal stem cell therapy for osteoarthritis: the critical role of the cell secretome. Front. Bioeng. Biotechnol. 7, 9.
Morici, L., Allémann, E., Rodríguez-Nogales, C., Jordan, O., 2024. Cartilage-targeted drug nanocarriers for osteoarthritis therapy. Int. J. Pharm. 666, 124843.
Moya, A., Paquet, J., Deschepper, M., Larochette, N., Oudina, K., Denoeud, C., et al., 2018. Human mesenchymal stem cell failure to adapt to glucose shortage and rapidly use intracellular energy reserves through glycolysis explains poor cell survival after implantation. Stem Cells 36 (3), 363–376.
Nakai, N., Kitai, S., Iida, N., Inoue, S., Nakata, K., Murakami, T., et al., 2020. Induction of Autophagy and changes in cellular Metabolism in Glucose Starved C2C12 Myotubes. J. Nutr. Sci. Vitaminol. (Tokyo) 66 (1), 41–47.
Nüchel, J., Tauber, M., Nolte, J.L., Mörgelin, M., Türk, C., Eckes, B., et al., 2021. An mTORC1-GRASP55 signaling axis controls unconventional secretion to reshape the extracellular proteome upon stress. Mol. Cell 81 (16).
Nuschke, A., Rodrigues, M., Wells, A.W., Sylakowski, K., Wells, A., 2016. Mesenchymal stem cells/multipotent stromal cells (MSCs) are glycolytic and thus glucose is a limiting factor of in vitro models of MSC starvation. Stem Cell Res Ther 7 (1), 179.
Park, J.S., Yi, S.W., Kim, H.J., Park, K.H., 2016. Receptor-mediated gene delivery into human mesenchymal stem cells using hyaluronic acid-shielded polyethylenimine/pDNA nanogels. Carbohydr. Polym. 136, 791–802.
Rose, B.J., Kooyman, D.L., 2016. A tale of two joints: the role of matrix metalloproteases in cartilage biology. Dis. Markers 2016, 4895050.
Salgado, J.C.S., Meleiro, L.P., Carli, S., Ward, R.J., 2018. Glucose tolerant and glucose stimulated β-glucosidases – a review. Bioresour. Technol. 267, 704–713.
Tonomura, H., Nagae, M., Takatori, R., Ishibashi, H., Itsuji, T., Takahashi, K., 2020. The potential role of hepatocyte growth factor in degenerative disorders of the synovial joint and spine. Int. J. Mol. Sci. 21 (22).
van Leeuwen, W., van der Krift, F., Rabouille, C., 2018. Modulation of the secretory pathway by amino-acid starvation. J. Cell Biol. 217 (7), 2261–2271.
Vonica, A., Bhat, N., Phan, K., Guo, J., Iancu, L., Weber, J.A., et al., 2020. Apcdd1 is a dual BMP/Wnt inhibitor in the developing nervous system and skin. Dev. Biol. 464 (1), 71–87.
Xiang, X.N., Zhu, S.Y., He, H.C., Yu, X., Xu, Y., He, C.Q., 2022. Mesenchymal stromal cell-based therapy for cartilage regeneration in knee osteoarthritis. Stem Cell Res Ther 13 (1), 14.
Xu, X., Zheng, L., Yuan, Q., Zhen, G., Crane, J.L., Zhou, X., et al., 2018. Transforming growth factor-β in stem cells and tissue homeostasis. Bone Res. 6, 2.
Yang, H., Zhou, Y., Ying, B., Dong, X., Qian, Q., Gao, S., 2024. Effects of human umbilical cord mesenchymal stem cell-derived exosomes in the rat osteoarthritis models. Stem Cells Transl. Med. 13 (8), 803–811.
Yao, Q., Wu, X., Tao, C., Gong, W., Chen, M., Qu, M., et al., 2023. Osteoarthritis: pathogenic signaling pathways and therapeutic targets. Signal Transduct. Target. Ther. 8 (1), 56.
Ying, J., Wang, P., Zhang, S., Xu, T., Zhang, L., Dong, R., et al., 2018. Transforming growth factor-beta1 promotes articular cartilage repair through canonical Smad and Hippo pathways in bone mesenchymal stem cells. Life Sci. 192, 84–90.
Zhao, M., Yang, M., Li, X., Hou, L., Liu, X., Xiao, W., 2021. Acid sphingomyelinase and acid β-glucosidase 1 exert opposite effects on interleukin-1β-induced interleukin 6 production in rheumatoid arthritis fibroblast-like synoviocytes. Inflammation 44 (4), 1592–1606.
Zhu, M., Tang, D., Wu, Q., Hao, S., Chen, M., Xie, C., et al., 2009. Activation of beta-catenin signaling in articular chondrocytes leads to osteoarthritis-like phenotype in adult beta-catenin conditional activation mice. J. Bone Miner. Res. 24 (1), 12–21.
Zou, J., Yang, W., Cui, W., Li, C., Ma, C., Ji, X., et al., 2023. Therapeutic potential and mechanisms of mesenchymal stem cell-derived exosomes as bioactive materials in tendon-bone healing. J. Nanobiotechnol. 21 (1), 14.